J|A|C|S
ARTICLES
Published on Web 03/21/2007

Tuning the Bergman Cyclization by Introduction of Metal Fragments at Various Positions of the Enediyne. Metalla-Bergman Cyclizations

Edyta M. Brzostowska,[†] Roald Hoffmann,*[,†] and Carol A. Parish[‡]

Contribution from the Department of Chemistry and Chemical Biology, Baker Laboratory, Cornell University, Ithaca, New York 14853, and Department of Chemistry, University of Richmond, Richmond, Virginia 23173

Received December 12, 2006; E-mail: rh34@cornell.edu

Abstract: We expand the scope of the Bergman cyclization by exploring computationally the rearrangement of two osmaenediynes and one rhodaenediyne. The three hypothetical metallaenediynes are constructed by substituting the 14-electron $Os(PH_3)_3$ fragment for the C fragment, or the 15-electron $Os(PH_3)_3H$ or $Rh(PH_3)_3$ fragments for the sp^2 CH fragment, of 3-ene-1,5-diyne. This replacement is guided by the isolobal analogy and previous metallabenzene chemistry. The rearrangement of osmaenediyne with an $Os(PH_3)_3$ fragment in place of C is exothermic by 3 kcal/mol (the parent Bergman reaction is computed to be endothermic by 5 kcal/mol) and associated with a significant decrease in the barrier to rearrangement to 13 kcal/mol (the E_a of the parent reaction computed at the same level of theory is 33 kcal/mol). The replacement of a CH by the isolobal analogue $Os(PH_3)_3H$ reduces the energy of activation for the rearrangement to 23 kcal/mol and produces a corresponding metalladiradical that is 8 kcal/mol less stable that the corresponding osmaenediyne. The activation energy corresponding to the rearrangement of the rhodaenediyne is the same as that of the organic parent enediyne. Interesting polytopal rearrangements of metallaenediynes and the diradical nature of the resulting intermediates are also explored.

Introduction

The Bergman cyclization of a 3-ene-1,5-diyne (called the parent enediyne) (**1**) to a 1,4-didehydrobenzene diradical (**3**), passing through a transition state (**2**) (Figure 1),[1] is remarkable in a number of ways. First, there is the reaction's history—a salutary example of how an intellectual challenge in a mechanistic organic setting turned out to be intimately involved in the workings of several naturally occurring antibiotics.[2] Second, this symmetry-allowed Cope reaction (or 2+2+2 cycloaddition) turns out to have a low activation energy. And, surprisingly, the reaction is only slightly endothermic (observed and computed energies are shown in Figure 1).[3] In a hydrocarbon environment, the diradical **3** often goes on to benzene by abstracting two hydrogens. This abstraction is implicated in the mode of biological action of enediynes.[2]

Some effort has gone into modifying the energetics of the reaction, with a concentration on modifications of the C_1-C_6 separation in the reactant to achieve an yne-to-yne end-to-end distance closer to the C_1-C_6 separation in the transition state.[2,4] This is a difficult task, because the reactant C_1-C_6 distance is 4.5 Å, while the transition state separation is 2.0 Å.[5] We set out to design a significant reduction in that distance by utilizing the isolobal analogy[6] in the construction of hypothetical organometallic molecules such as **4** and **5**. Given typical geometries at metals, one could imagine in such molecules C−M−C and M−M−C angles of ∼90°, which in turn would bring the ends of the yne fragments closer together.

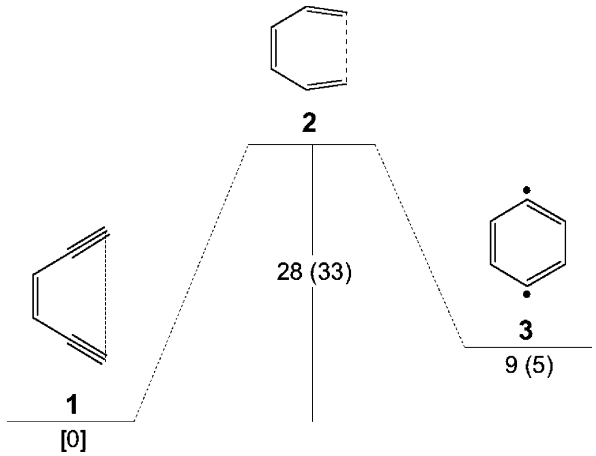

Figure 1. Schematic potential energy surface of the Bergman rearrangement of enediyne **1**. Experimental (and theoretical B3LYP/SDD) values are given in kcal/mol.

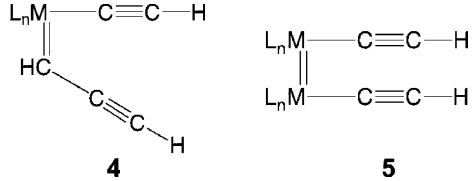

4 **5**

[†] Cornell University.
[‡] University of Richmond.

(1) Jones, R. R.; Bergman, R. G. *J. Am. Chem. Soc.* **1972**, *94*, 660−661.
(2) Nicolaou, K. C.; Dai W.-M. *Angew. Chem., Int. Ed. Engl.* **1991**, *30*, 1387−1417 and references therein.
(3) (a) Bergman, R. G. *Acc. Chem. Res.* **1973**, *6*, 25−31. (b) Roth, W. R.; Hopf, H.; Horn, C. *Chem. Ber.* **1994**, *127*, 1765−1769.

Scheme 1

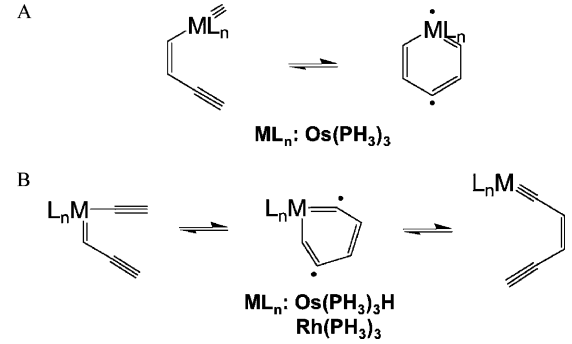

The computational outcome of the investigation of systems of type **5** will be reported elsewhere;[7] here we detail the interesting results of a study of analogues of the Bergman reaction with just one ML_n fragment substituted for a CH or C group.

Metalla-Bergman Cyclizations

What metal fragment might serve to replace C or CH in the Bergman rearrangement? The isolobal analogy[6] is a reasonable guide to such maneuvers across the organic−inorganic divide. An isolobal analogue of an enediyne, a metallaenediyne, could, for example, be obtained by substitution of the four-electron C fragment in **1** by a 14-electron ML_n metal fragment (Scheme 1A), or the five-electron CH group could be replaced by a 15-electron ML_n (Scheme 1B).

In our specific choice of ML_n fragments, we were influenced by the metallabenzenes in the literature.[8] These include three classes of metallabenzenes examined theoretically by Thorn and Hoffmann,[9] the first stable osmabenzenes isolated by Roper,[10,11] those proposed by Jia as intermediates in the synthesis of osmabenzynes,[12] and iridabenzenes synthesized by Bleeke.[13] For the purpose of our studies, we then decided to use the 14-electron $[Os(PH_3)_3]$ fragment to replace a 4-electron C fragment and, separately, 15-electron $[Os(PH_3)_3H]$ and $[Rh(PH_3)_3]$ to replace the C−H fragment of enediyne **1**.

The thought was that such transformation might potentially lower the activation energy, E_a, of the Bergman cyclization by (i) a decrease in the distance *d* between acetylides of enediyne **1** (through a potential CMC right angle, Scheme 1B) and/or (ii) potential stabilization of a radical at the transition metal center (Scheme 1A). We report here electronic structure calculations for the cyclization of metallaenediynes. As we will see, there is indeed a significant decrease of the activation energy, E_a, in some of these reactions.

It should be made clear at the outset that our computations do not address important questions of stability and safety regarding organometallics as therapeutic agents. We rather investigate how the organometallic fragment affects the crucial energetics of the underlying reaction.

Computational Details

Density functional calculations were performed with the Gaussian 03 program[14] using the restricted B3LYP[15] functional with an SDD basis set (D95V: Dunning−Huzinaga valence double-ζ[16] on H, C, O, P, and Cl and Stuttgart−Dresden[17] for effective core potential approximations on Rh and Os) for singlet-state metallaenediynes, transition states, and metallabenzenes. An unrestricted B3LYP functional with an SDD basis set was used for singlet- and triplet-state metallabenzynes. The often-used hybrid B3LYP functional has gained a reputation as the one of the most accurate methods in studies of transition metal compounds and their reactions[18,19] and has been shown to be superior to the pure BLYP functional[20] for the calculations of diradicals by Cremer et al.[21] and Schreiner and co-workers.[22c] Recently, the B3LYP functional, in combination with the SDD basis set, was applied to the study of $M_2(O_2CMe)_4$ (M = Mo and W) paddlewheel complexes and their radical cations.[23] Finally, our ability to reproduce the experimental and computational results reported by Jia for *o*-osmabenzynes[12] with B3LYP/SDD (data not shown here) convinced us to apply it for the purpose of the present study.

All compounds optimized to well-defined minima or maxima on their potential energy surfaces, as verified by frequency analyses. Furthermore, all predicted transition states were characterized using intrinsic reaction coordinate calculations.[24] All density functional theory (DFT) calculations were performed with an integration grid equal to "UltraFine", recommended for molecules containing many tetrahedral centers.[24] All geometry optimizations were carried out with no symmetry restrictions. The unrestricted DFT geometry optimizations of singlet and triplet metallabenzynes were started with a wave function with broken symmetry (keyword guess = (mix,always) in the route section).[24]

For the visualization of the optimized structures and of molecular orbitals (isovalue for surfaces = 0.06 and 0.08), the GaussView (version 3.09) package was used.[25]

(4) (a) Nicolaou, K. C.; Smith, A. L. *Acc. Chem. Res.* **1992**, *25*, 497−503. (b) Warner, B. P.; Millar, S. P.; Broene, R. D.; Buchwald, S. L. *Science* **1995**, *269*, 814−816. (c) Kim, Ch.-S.; Russell, K. C. *J. Org. Chem.* **1998**, *63*, 8229−8234. (d) Cramer, C. J. *J. Am. Chem. Soc.* **1998**, *120*, 6261−6269. (e) Benites, P. J.; Rawat, D. S.; Zaleski, J. M. *J. Am. Chem. Soc.* **2000**, *122*, 7208−7217. (f) König, B. *Eur. J. Org. Chem.* **2000**, 381−385. (g) König, B.; Pitsch, W.; Klein, M.; Vasold, R.; Prall, M.; Schreiner, P. R. *J. Org. Chem.* **2001**, *66*, 1742−1746. (h) Prall, M.; Wittkopp, A.; Fokin, A. A.; Schreiner, P. R. *J. Comput. Chem.* **2001**, *22*, 1605−1614. (i) Kraka, E.; Cremer, D. *J. Comput. Chem.* **2001**, *22*, 216−229. (j) Basak A.; Mandal, S.; Bag, S. S. *Chem. Rev.* **2003**, *103*, 4077−4094. (k) Zeidan, T. A.; Manoharan, M.; Alabugin, I. V. *J. Org. Chem.* **2006**, *71*, 954−961. (l) Zeidan, T. A.; Kovalenko, S. V.; Manoharan, M.; Alabugin, I. V. *J. Org. Chem.* **2006**, *71*, 961−975. (m) Maretina, I. A.; Trofimov, B. A. *Russ. Chem. Rev.* **2006**, *75*, 825−845.
(5) (a) Calculated by using B3LYP/SDD, with the same functional and basis as for the metal-containing molecules studied in this paper. (b) Grafenstain, J.; Hjerpe, A. M.; Kraka, E.; Cremer, D. *J. Phys. Chem. A* **2000**, *104*, 1748−1761.
(6) Hoffmann, R. *Angew. Chem., Int. Ed. Engl.* **1982**, *21*, 711−724.
(7) To be published soon.
(8) Landorf, C. W.; Haley, M. M. *Angew. Chem., Int. Ed.* **2006**, *45*, 3914−3936.
(9) Thorn, D. L.; Hoffmann, R. *Nouv. J. Chim.* **1979**, *3*, 39−45.
(10) Elliott, G. P.; Roper, W. R.; Waters, J. M. *J. Chem. Soc., Chem. Commun.* **1982**, 811−813.
(11) Elliott, G. P.; McAuley, N. M.; Roper, W. R. *Inorg. Synth.* **1989**, *26*, 184−189.
(12) Jia, G. *Acc. Chem. Res.* **2005**, *37*, 479−486.
(13) Bleeke, J. R. *Chem. Rev.* **2001**, *101*, 1205−1227.
(14) Frisch, M. J.; et al. *Gaussian 03*, Revision B.04; Gaussian, Inc.: Pittsburgh, PA, 2003.
(15) Becke, A. D. *J. Chem. Phys.* **1993**, *98*, 5648−5652.
(16) Dunning, T. H., Jr.; Hay, P. J. In *Modern Theoretical Chemistry*; Schaefer, H. F., III, Ed.; Plenum: New York, 1976; Vol. 3, p 1.
(17) Fuenteabla, P.; Preuss, H.; Stoll, H.; Szentpaly, L. *Chem. Phys. Lett.* **1989**, *89*, 418.
(18) Niu, S.; Hall, M. B. *Chem. Rev.* **2000**, *100*, 353−405.
(19) Ziegler, T.; Autschbach, J. *Chem. Rev.* **2005**, *105*, 2695−2722.
(20) Lee, C.; Yang, W.; Parr, R. G. *Phys. Rev. B* **1988**, *37*, 785−789.
(21) Gräfenstain, J.; Kraka, E.; Filatov, M.; Cremer, D. *Int. J. Mol. Sci.* **2002**, *3*, 360−394.
(22) (a) Cramer, C. J. *Essentials of Computational Chemistry Theories and Models*, 2nd ed.; John Wiley & Sons, Inc.: New York, 2005. (b) Jensen, F. *Introduction to Computational Chemistry*; John Wiley & Sons, Inc.: New York, 1999. (c) Schreiner, P. R.; Navarro-Vazquez, A.; Prall, M. *Acc. Chem. Res.* **2005**, *38*, 29−37.
(23) Chisholm, M. H.; D'Acchioli, J. S.; Pate, B. D.; Patmore, N. J.; Dalal, N. S.; Zipse, D. J. *Inorg. Chem.* **2005**, *44*, 1061−1067.
(24) Fisher, Æ.; Frisch, G. W.; Trucks, G. W. *Gaussian 03 User's Reference*; Gaussian, Inc.: Pittsburgh, PA, 2003.
(25) Dennington, R., II; Keith, T.; Millam, J.; Eppinnett, K.; Hovell, W. L.; Gilliland, R. *GaussView*, Version 3.09; Semichem, Inc.: Shawnee Mission, KS, 2003.

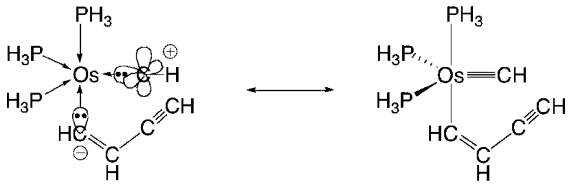

Figure 2. Formal construction of the bonding in osmaenediyne **6**.

Metalla-Bergman Cyclization of an Osmaenediyne

Consider the osmaenediyne **6**. Aside from the three PH_3 groups, the ligands at osmium are formally a vinylic eneyne anion (**:**CH═CH−C≡C−H)$^-$ and a CH carbyne.[26] If the carbyne is viewed (purely formally) as a 2-electron ligand, it is **:**CH^+. The Os≡CR triple bond is achieved by back-donation[26] of two electron pairs from the d orbitals on Os to the available empty p orbitals of the carbyne (Figure 2).

The osmaenediyne is an 18-electron d^8 five-coordinate ML_5 molecule. A trigonal bipyramid at Os is expected, and indeed an initial optimization of a trial geometry confirmed this. Of course, this coordination geometry raises a number of stereochemical possibilities: isomeric trigonal bipyramids and square pyramids interconverting via the Berry pseudorotation[27] or other polyhedral permutational processes.[28]

We began by examining the four isomeric trigonal bipyramids (Figure 3A). Three of them survived optimization, whereas the fourth (as well as all square pyramidal starting structures that we examined) collapsed to one of the remaining isomers, **6**, **6′**, and **6″**, shown in Figure 3B. For clarity, in Figure 3B, only the P of the PH_3 group is shown. The color code we use is maintained throughout this section.

The global minimum **6** was chosen for further reaction. The geometry of **6** is an approximate trigonal bipyramid at the Os, angular parameter $\tau = 0.7$,[29] with CH equatorial and the eneyne fragment axial. Important for our strategy, the (E)C−Os−CH angle is 95°. This decreases the distance between the acetylenes to 3.31 Å (compared to 4.5 Å in **1**). Certain points on the computed potential energy surface (PES) corresponding to the rearrangement of metallaenediyne **6** are shown in Figure 4.

The computed energy barrier of the metalla-Bergman rearrangement of **6** is, in fact, reduced to 13 kcal/mol, to be compared to the experimentally determined (28 kcal/mol)[3] and theoretically computed (33 kcal/mol)[5a] energy of activation for the all-hydrocarbon parent **1** (Figure 1). The metalla-Bergman rearrangement of **6** is also computed to be slightly exothermic, $\Delta E = -3$ kcal/mol.

The product of the rearrangement, singlet osmabiradical **8** ($\langle S^2 \rangle = 0.0$),[22,30] also has a distorted trigonal bipyramidal geometry (angular parameter $\tau = 0.5$[29]). The C−C bond distances in **8** range between 1.37 and 1.47 Å, and the ring is slightly nonplanar, making **8** chiral. The barrier to its racemization is computed as only 4 kcal/mol.[31]

Should we make something of the localization of C−C bonds in this osmabenzyne **8**? It should be good to know the extent of localization in metallabenzenes.[8,13] This is not easy to come by, as many of the known compounds are highly substituted in an asymmetric way. A range of C−C distances from 1.3X to 1.4Y Å is seen in one set of structures.[8,13] A calculation on **8** with two H's added (to be reported later) gives quite equalized C−C distances, 1.41 Å. By comparison, **8** shows more bond localization and presumably less aromaticity. It is interesting to note that the computed C−C distances in **8** (1.47, 1.37 Å) are close to those calculated for *p*-benzyne (1.47, 1.35 Å).[32]

Note that, in structure **8**, we give the C−C and M−C distances in the ring but graphically connect the atoms only by single lines. From the distances, it is clear that there is some multiple bond character (and some localization as well, cf. 1.37 vs 1.47 Å), but we would rather not enter here a discussion—not an easy one—of the bond order of these bonds. The convention of single lines in diradicals is followed throughout this paper.

The accuracy of the calculations with the hybrid functional B3LYP and the SDD basis set was tested and compared to results obtained with the pure BLYP functional and the same basis set. This test was prompted by the fact that the Bergman cyclization may be viewed as a Cope rearrangement,[33,34] and, in the definitive study of the Cope rearrangement of 1,5-hexadiene, Staroverov and Davidson showed that UB3LYP may lead to spurious diradical (1,4-diyl) intermediates.[35] Both methods were also tested in combination with the LANL2DZ basis set[16] developed to study organometallic compounds. The results of our calculations are reported in the Table 1.

The metalla-Bergman rearrangement of **6** is exothermic, and the energy barrier is in the range 9−13 kcal/mol in all four cases studied.[36] The BLYP/SDD method predicted the *para*-osmadiradical **8** to have a square pyramidal geometry (angular

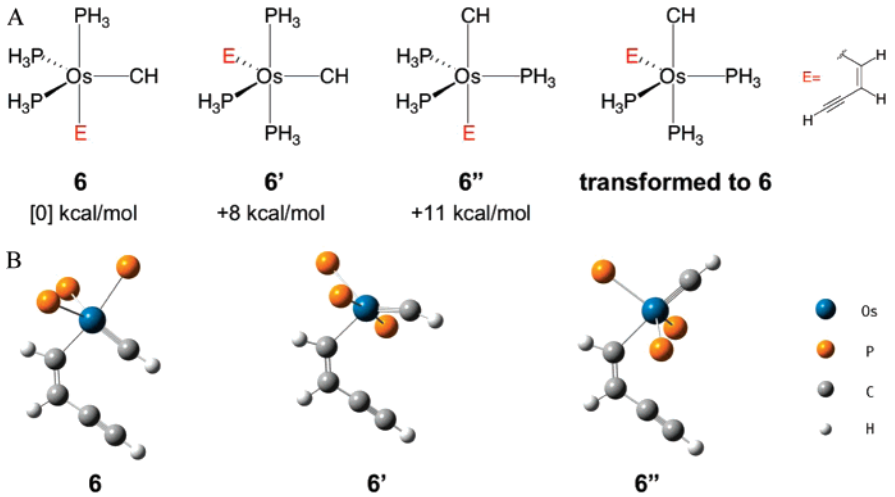

Figure 3. (A) Isomeric trigonal bipyramidal structures for **6**. (B) Optimized isomeric trigonal bipyramids **6**, **6′**, and **6″**.

Table 1. Influence of the Functional and Basis Set on Some of the Results Computed for Rearrangement of **6**

method/basis set	**6** (kcal/mol)	**7** TS (kcal/mol)	**8** singlet (kcal/mol)	geometry of **8**	$\langle S^2\rangle^a$ of **8**	τ^b of **8**
B3LYP/SDD	[0]	13	−3	distorted tbp[c]	0.0	0.5
BLYP/ SDD	[0]	10	−8	sp[d]	0.82	0.1
B3LYP/LANL2DZ	[0]	12	−4	distorted tbp[c]	0.0	0.5
BLYP/ LANL2DZ	[0]	9	−6	distorted tbp[c]	0.0	0.5

[a] Spin-squared expectation value.[22] [b] Angular parameter.[29] [c] Trigonal bipyramid. [d] Square pyramid.

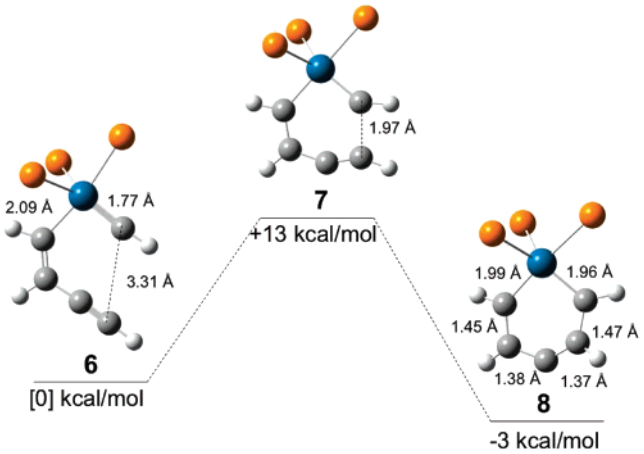

Figure 4. Metalla-Bergman cyclization of **6**. The atom color code is the same as in Figure 3.

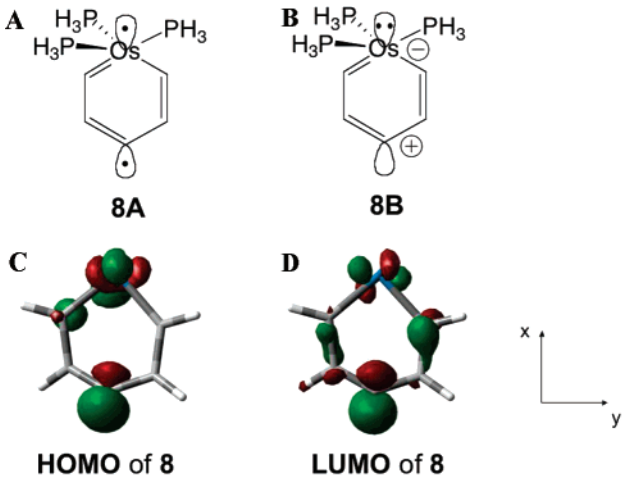

Figure 5. (A) Diradical and (B) zwitterionic valence structures for **8**. (C,D) HOMO and LUMO of **8** (the two localized orbitals of HOMO and LUMO, occupied by α and β electrons, are equivalent in phase and shape); the three PH_3 ligands at the Os center were removed for clarity (isovalue for surfaces = 0.08).

parameter $\tau = 0.1$[29]) with $\langle S^2\rangle = 0.8$,[22] suggesting spin contamination from mixing of the singlet and low-lying triplet states. All other methods predicted a trigonal bipyramidal geometry with $\langle S^2\rangle = 0.0$.[22] The satisfying independence of our results on functional and basis set led us to continue our studies of the metalla-Bergman rearrangement with the B3LYP/SDD level of theory.

Scheme 1, our blueprint for the metalla-Bergman reaction, implies that **8** is a *p*-osmabenzyne, a diradical with one radical site localized on the metal, **8A** (Figure 5). One could also come up with an alternative valence structure, **8B**. This features a cationic center at the *para*-carbon and an 18-electron complex at the metal. It is not easy to assign a preference to one or another valence structure, but some insight may be gained by a comparison to the highest occupied and lowest unoccupied molecular orbitals (HOMO and LUMO) of the parent *p*-benzyne shown in Figure 6.[22c,37−40]

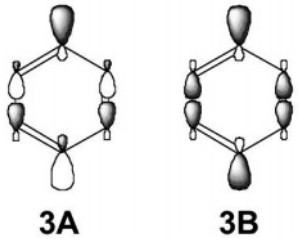

Figure 6. HOMO (**3A**) and LUMO (**3B**) of *p*-benzyne.

The phases of the orbitals follow from the through-bond coupling that underlies the electronic structure of the diradical. The HOMO and LUMO of **8**, shown in Figure 5, are not expected to be as simple as (**3A** + **3B**). In fact, they emerge, as Figure 5C,D shows, as combinations of a lobe, mainly p_x, on the *para*-C center, and a d orbital on the metal. In the HOMO, the metal orbital can be described as z^2-y^2, and in the LUMO, it can be described as a mixture of z^2-y^2 and *yz*, in the specified coordinate system. Because the MC_5 ring in **8** is not planar, there is some mixing of σ and π character evident in these orbitals.

(26) Crabtree R. H. *The Organometallic Chemistry of the Transition Metals*, 4th ed.; John Wiley & Sons, Inc.: New York, 2005.
(27) (a) Berry, R. S. *J. Chem. Phys.* **1960**, *32*, 933−938. (b) Bartell, L. S.; Kuchitsu, K.; deNeui, R. J *J. Chem. Phys.* **1961**, *35*, 1211−1218.
(28) Rzepa, H. S.; Cass, M. E. *Inorg. Chem.* **2006**, *10*, 3958−3963.
(29) An angular parameter τ maybe used to classify the geometry of pentacoordinate compounds. It is defined as $\tau = (\alpha - \beta)/60$, where α and β are the two largest L−M−L angles, and $\alpha \geq \beta$. A perfect trigonal bipyramid has $\alpha = 180°$ and $\beta = 120°$, thus $\tau = 1$, whereas in a perfect square pyramid $\alpha = \beta$, i.e., $\tau = 0$. (a) Addison, A. W.; Rao, T. N.; Reedijk, J.; Rijn, v. J.; Verschoor, G. C. *J. Chem. Soc., Dalton. Trans.* **1984**, 1349−1356. (b) Alvarez, S.; Llunell, M. *J. Chem. Soc., Dalton. Trans.* **2000**, 3288−3303.
(30) $\langle S^2\rangle$ values for open-shell singlet and triplet structures of the trigonal bipyramid **8** are 0.00 and 2.03, respectively, whereas $\langle S^2\rangle$ values corresponding to singlet and triplet of **8′** are 0.00 and 2.04. $\langle S^2\rangle$ values for open-shell singlet and triplet structures of **11** are 0.97 and 2.02, respectively, whereas $\langle S^2\rangle$ values corresponding to singlet and triplet of **11′** are 0.00 and 2.02. Finally, $\langle S^2\rangle$ values for open-shell, singlet and triplet structures of **15** are 0.00 and 2.02, whereas $\langle S^2\rangle$ values corresponding to singlet and triplet of **15′** are 0.13 and 2.02, respectively.
(31) Details can be found in the Supporting Information.
(32) Shao, Y.; Head-Gorgon, M.; Krylow, A. I. *J. Chem. Phys.* **2003**, *118*, 4807−4818.
(33) Houk, K. N.; Li, Y.; Evanseck, J. D. *Angew. Chem., Int. Ed. Engl.* **1992**, *31*, 682−708.
(34) Hopf, H. *Classics in Hydrocarbon Chemistry*; Wiley-VCH: Weinheim, Germany, 2000.
(35) Staroverov, V. N.; Davidson, E. R. *J. Mol. Struct. (Theochem)* **2001**, *573*, 81−89.
(36) The potential energy surfaces for the rearrangement of osmaenediyne **6** computed with BLYP/SDD, B3LYP/LANL2DZ, and BLYP/LANL2DZ are reported in the Supporting Information.
(37) Albright, T. A.; Burdett, J. K.; Whangbo, M.-H. *Orbital Interactions in Chemistry*; John Wiley & Sons, Inc.: New York, 1985.
(38) Hoffmann, R. *Acc. Chem. Res.* **1971**, *4*, 1−9.
(39) These orbitals are those expected for a restricted HF solution. The actual α and β spin orbitals in an unrestricted HF calculations are localized on one or the other *p*-benzyne carbon. This is not true for the HOMO of **8**, where the UB3LYP calculations yield orbitals identical for α and β spins (shown in Figure 7).
(40) Borden, W. T., Ed. *Diradicals*; John Wiley & Sons, Inc.: New York, 1982.

An argument for a zwitterionic valence structure (Figure 5B) might be found in the natural bond orbital (NBO) charge distribution in the singlet **8** (not shown here in detail), which indicates positive charge at the carbon *para* to the metal, but the charge differential relative to the NBO charges for *p*-benzyne is not excessive (see Supporting Information).

It is not simple to decide whether a given species is a diradical.[41,42] A reviewer has properly pointed out that "the issue of whether multi-reference wave functions are more appropriate is always lurking under the surface." And whether one has a diradical or a zwitterion may depend totally on the solvent. Until better measures of diradical character are agreed on, we prefer on balance the diradical formulation **8A**.

The triplet state of **8** is a significantly different structure than the singlet; the singlet is a distorted trigonal bipyramid with angular parameter $\tau = 0.5$,[29] whereas the triplet state optimizes to a square pyramidal geometry ($\tau = 0.0$[29]), 11 kcal/mol more stable than the singlet. The vertical singlet−triplet energy gap (at the singlet geometry), ΔE_{S-T}, is 9.8 kcal/mol.[43]

Given our experience with the PES of phosphoranes and Fe(CO)$_5$,[44,45] we are also led to consider another process for polytopal rearrangements in **8**, called turnstile rotation.[46] A series of calculations, not reported in detail here, revealed a high-energy barrier (>40 kcal/mol) for aligning the Os(PH$_3$)$_3$ three-fold rotor with the two-fold OsC$_5$H$_4$ axis necessary for a turnstile rotation to occur. So this mechanism for polytopal rearrangement of **8** does not appear to be realistic.

Searching for alternative structures of the biradical, we did discover another minimum, **8′**.[47] As the figure shows, the

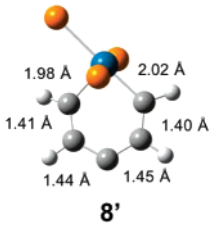

geometry of **8′** is an interesting flat square pyramid (angular parameter $\tau = 0.1$[29]), apparently creating the "space" for a radical lobe.[48] Singlet **8′**[30,43] is 2 kcal/mol above **8** but, as a vibrational analysis shows, exists as its own local energy minimum. Square pyramid **8′** can undergo interconversion to its enantiomer with relative ease (6 kcal/mol, Figure 7). The process involves a decrease of the C(H)−Os−P angle; the transition state occurs when one PH$_3$ moves approximately 42° (Figure 7).

Returning to the relationship of this alternative geometry to **8**, the activation energy for the **8′** → **8** process is computed as

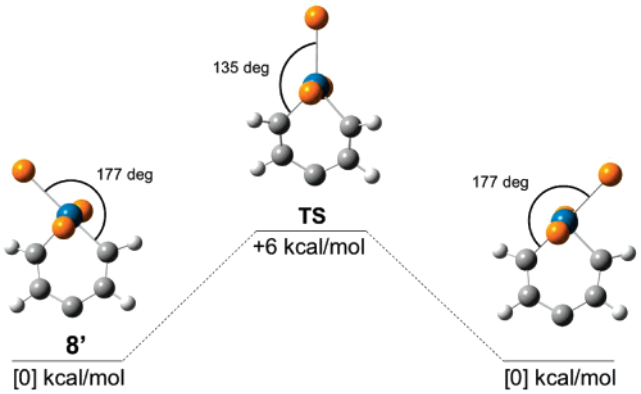

Figure 7. Interconversion of square pyramid **8′**.

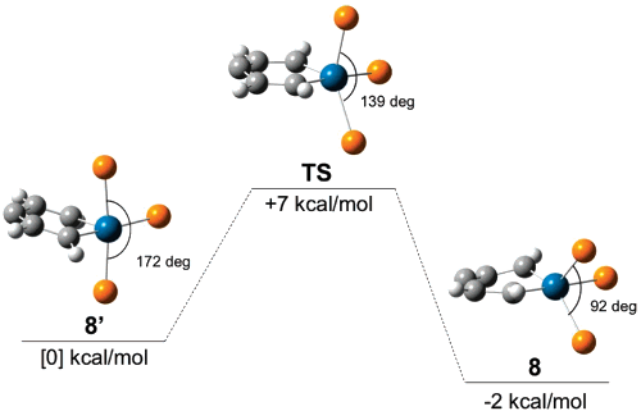

Figure 8. Transformation of square pyramid **8′** to its isomer, trigonal bipyramid **8**.

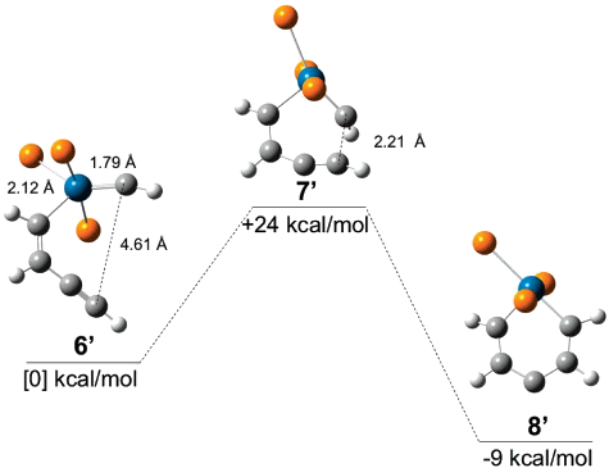

Figure 9. Metalla-Bergman rearrangement of **6′**.

7 kcal/mol; the reaction path is associated with a decrease of the P−Os−P angle from 172° in **8′** to 92° in **8** (Figure 8). The bond lengths in **8′** are more uniform, and longer, than those in **8**, suggesting less electron density but more aromaticity in the more planar hydrocarbon ring.

Interestingly, further studies revealed that **8′** could also be formed by an exothermic metalla-Bergman cyclization of **6′** (another of the trigonal bipyramidal isomers of **6**), with computed activation energy of 24 kcal/mol (Figure 9).

It is clear that the potential energy landscape surrounding the metalla-Bergman reactions of osmaenediynes is not simple. First, polytopal rearrangements of reactants and products

(41) Jung, Y.; Head-Gordon, M. *Chem. Phys. Chem.* **2003**, *4*, 522−525.
(42) Seierstad, M.; Kinsinger, C. R.; Cramer, C. J. *Angew. Chem., Int. Ed.* **2002**, *41*, 3894−3896.
(43) The energy and $\langle S^2 \rangle$ of singlet **8**, **8′**, **11**, **11′**, and **15** and triplet (from singlet geometry) as well as energy and $\langle S^2 \rangle$ of singlet (from triplet geometry) and triplet are provided in the Supporting Information.
(44) Hoffmann, R.; Howell, J. M.; Muetteries, E. L. *J. Am. Chem. Soc.* **1972**, *94*, 3047−3058.
(45) Rossi, A. R.; Hoffmann, R. *Inorg. Chem.* **1975**, *14*, 365−374.
(46) Gillespie P.; Hoffman, P.; Klusacek, H.; Marquarding, D.; Pfohl, S.; Ramirez, F.; Tsolis, E. A.; Ugi, I. *Angew. Chem., Int. Ed. Engl.* **1971**, *10*, 687−715.
(47) Note again, as we discussed in the text around structure **8**, that we avoid a discussion of the bond order of the various bonds but do give their computed lengths.
(48) The HOMO and LUMO of singlet **8**, **8′**, **11**, **11′**, and **15** are shown in the Supporting Information.

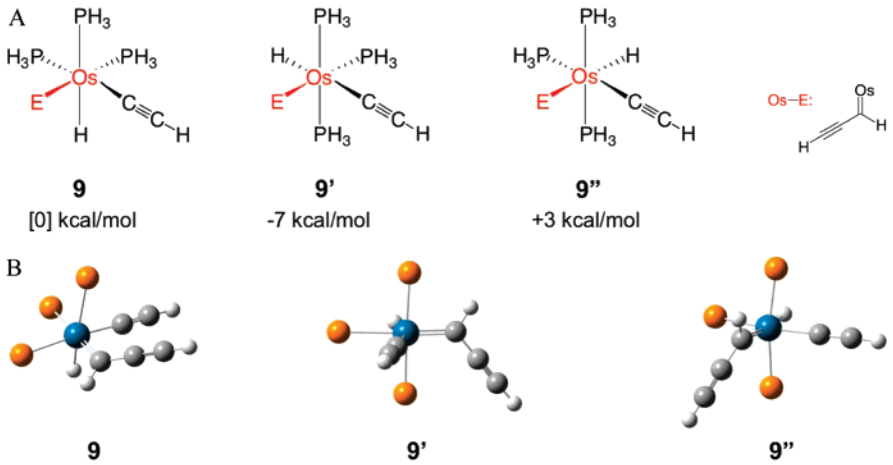

Figure 10. (A) Starting octahedral isomers of **9**. (B) Optimized structures of metallaenediynes **9**, **9′**, and **9″**. The atom color code is that of Figure 3, with only the P atom (orange) of PH_3 shown.

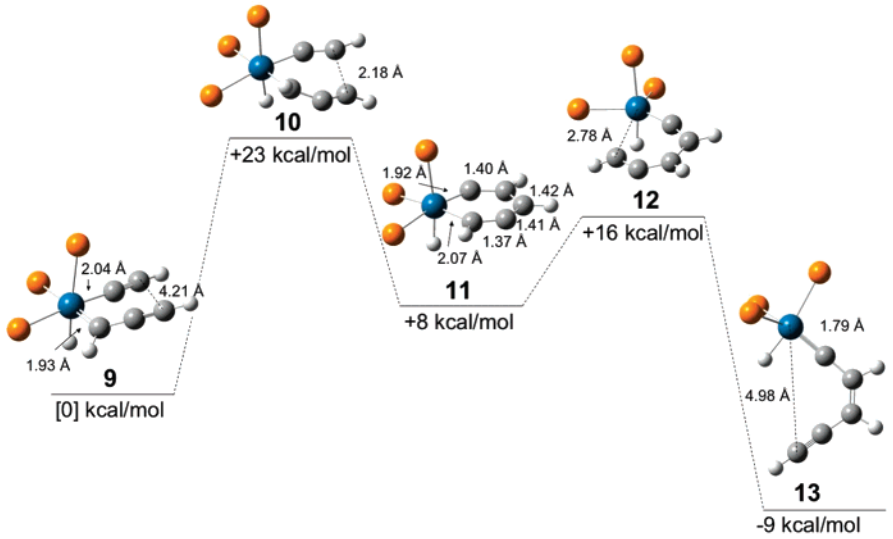

Figure 11. Computed geometries and energies of stationary points in the metalla-Bergman cyclization of **9**.

introduce substantial geometrical freedom, even at high energetic costs. Second, the metal analogues of the *p*-benzyne intermediate have electronic degrees of freedom available to them that will take theoretical investigations of some depth to fix reliably. In this study, we are just sketching out the rough features of this complex landscape.

Metalla-Bergman Cyclization of Another Osmabenzyne

In the second case investigated (Scheme 1B), we try replacing a CH of the ene group of the enediyne **1** by the isolobal 15-electron fragment $Os(PH_3)_3H$. The metalla-Bergman rearrangement is here initiated from an 18-electron complex (**9**) of approximately octahedral geometry. In this case, a formal d^6 Os^{2+} is surrounded by six ligands: three phosphines, one hydride, an acetylide $(:C{\equiv}CH)^-$, and a formal carbene, :CH−C≡CH. Here, d→p back-bonding leads to an Os=C double bond.[26]

There are three possible geometric isomers of **9**, one of which is chiral (Figure 10A). As may be seen in Figure 10B, in the equilibrium geometry of the lowest energy isomer (**9′**) and the highest energy isomer (**9″**), the two acetylides which need to interact are not coplanar: the (sp)C−(sp^2)C−Os−(sp)C dihedral angle is computed to be 90° and 107°, respectively, and the yne termini are far apart (6.05 Å in **9′** and 6.16 Å in **9″**). In the case of isomer **9** and its enantiomer, the (sp)C−(sp^2)C−Os−(sp)C dihedral angle is reduced to 30°. We studied further **9** and **9′**.

In the starting structure **9**, the C−Os−C(H) angle is 93°; however, the yne−yne end-to-end distance *d* is computed to be 4.21 Å. This is the consequence of the greater Os=C distance (1.93 Å compared to C=C). The activation energy for the metalla-Bergman rearrangement of **9** is 23 kcal/mol (Figure 11). The reaction **9**→[**10**]‡→**11** is endothermic (ΔE = 8 kcal/mol).

The product of the rearrangement is singlet osmabenzyne **11**. This intermediate has its unpaired electrons located on two *para*-carbons.[48] A valence structure of **11** can be formulated which makes it an 18-electron complex, consistent with approximately octahedral geometry at the metal. The ring of osmabenzyne **11** emerges almost planar and quite "aromatic", as judged by its relative bond equalization (Figure 11)—the C−C bond distances in **11** vary from 1.37 to 1.42 Å. The triplet state of osmabenzyne, calculated from the geometry of singlet **11**, is less stable than the singlet, ΔE_{S-T} = 2.6 kcal/mol.[43]

As Scheme 1B shows, diradical **11** can either undergo a retro-metalla-Bergman cyclization to regenerate the starting structure or ring-open in a distinct way to **13**). The retro-metalla-Bergman

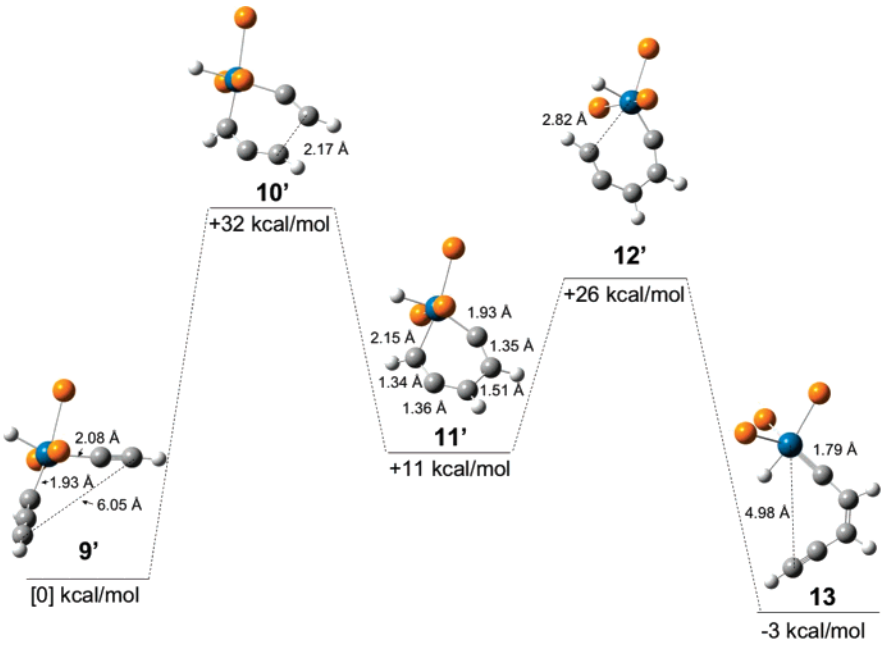

Figure 12. Metalla-Bergman cyclization of **9′**; energies and geometries of stationary points.

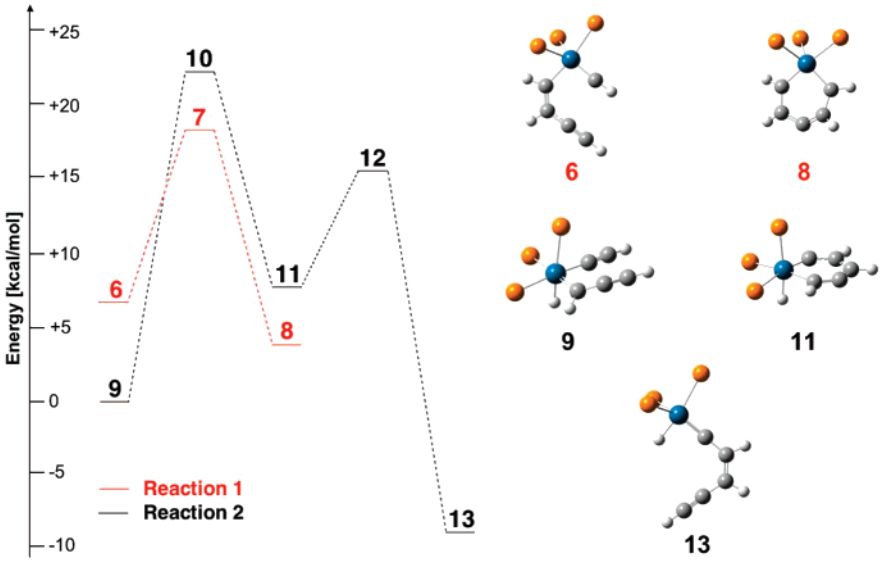

Figure 13. Metalla-Bergman rearrangement of the osmaenediyne **6** vs the metalla-Bergman rearrangement of osmaenediyne **9**; a comparison on the same energy scale. Energy is given in kcal/mol.

rearrangement has an energy barrier of 15 kcal/mol, while the ring-opening to **13** costs only 8 kcal/mol. The rearrangement of **11** to **13** involves an octahedral-like transition state (**12**). Compound **13** is an 18-electron distorted trigonal bipyramid (angular parameter $\tau = 0.7$[29]) at the metal center. Pentacoordinate complex **13** is also the lowest energy isomer[49] among four possible trigonal bipyramids and four square pyramids rearranging via a Berry pseudorotation mechanism.

The barrier to ring formation in the metalla-Bergman rearrangement of **9′**, computed as 32 kcal/mol, is 8 kcal/mol higher than that of **9** (Figure 12). The increase in activation energy appears to originate from the cost of twisting the acetylide around the Os=C(H) bond so as to get the ring carbons into a plane. The energy required to rotate the acetylide to achieve the (sp)C−(sp^2)C−Os−(sp)C dihedral angle of 40°, the same angle as in transition state **9′**, is computed as 13 kcal/mol.

Comparing Two Possible Reactions of Osmaenediynes

All the molecules in reactions 1 and 2 (shown in Figure 13) have the same stoichiometry; to put it another way, **6** and **9** are structural isomers. Thus, we are able to compare both processes on the same energy scale (see Figure 13; we put the energy zero arbitrarily at the energy of **9**). Interestingly, the starting structure of reaction 1, compound **6**, is 7 kcal/mol less stable than compound **9**, whereas the osmaenediyne **13** obtained in the ring-opening of **11** (reaction 2) is 16 kcal/mol more stable than metallaenediyne **6**. Both compounds **6** and **13** are trigonal bipyramids. It appears that placing Os(PH$_3$)$_3$H at the acetylenic

(49) Eight potential isomers arising in the Berry pseudorotation of **13** were optimized. Two trigonal bipyramids and two square pyramids collapsed to complex **13** ([0] kcal/mol). Three other isomers (including one trigonal bipyramid and two square pyramids) transformed into a trigonal bipyramidal structure 7 kcal/mol less stable than **13**. One optimized trigonal bipyramid was +11 kcal higher in energy than **13**.

terminus reduces significantly the steric hindrance in **13** and makes it the most stable among all compounds studied.

Finally, metallabenzyne **8** of reaction 1 is 4 kcal/mol more stable than **11** of reaction 2. One implication might be that the metal fragment ($Os(PH_3)_3$) in **8** is able to stabilize an unpaired electron better than the C atom in **11**.

Metalla-Bergman Cyclization of a Rhodaenediyne

The moderately successful decrease of the energy of activation of the metalla-Bergman cyclization of **9** (E_a = 23 kcal/mol relative to E_a = 33 kcal/mol for the parent enediyne) led us to try replacement of a CH group by another isolobal analogue, a 15-electron metal fragment, $Rh(PH_3)_3$. This led to rhodaenediyne **14**.

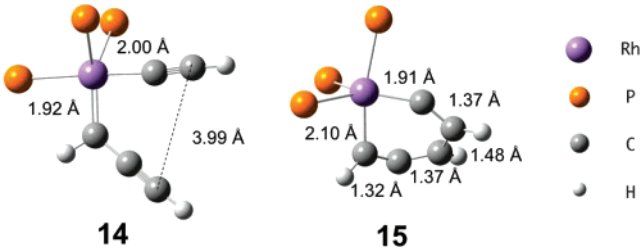

The outcome of these calculations is given in detail in the Supporting Information. A brief summary is that the PES resembles that of Figure 12, except that the *p*-rhodabenzyne **15**[43,48] is somewhat more stable (7 kcal/mol, relative to starting material), and the forward metalla-Bergman reaction is still easier (5 kcal/mol, Figure 3 in Supporting Information) than for $ML_n{=}Os(PH_3)_3H$ (15 kcal/mol, Figure 12). The activation energy for the metalla-Bergman reaction of **14** is, however, computed to be high, 33 kcal/mol.

Ortho-Metallabenzynes

Para-metallabenzynes **8**, **11**, and **15** belong to a novel class of compounds, not yet synthesized. They are isomers of *ortho*-metallabenzynes. *o*-Osmabenzynes have been synthesized and characterized.[12,50] We found it interesting to compare the energies of *para*- and *ortho*-metallabenzynes **8** and **16**.

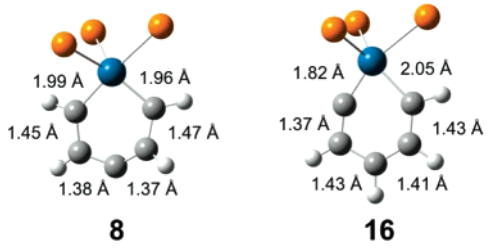

We calculated that the *o*-osmabenzyne **16** is 48 kcal/mol more stable than the *para* isomer **8**. Compound **16**, unlike **8**, is of C_s geometry, with an almost planar ring. (Singlet *o*-osmabenzyne **16** is 21 kcal/mol more stable than triplet.) The C−C bond distances in **16** are in the range of 1.37−1.43 Å. The Os−C length in **16** is 1.82 Å, whereas Os−C(H) is 2.05 Å. The bond lengths in **8** have been discussed above. The ones in **16** appear to be more equalized, but it is still difficult to make a judgment

(50) Hung, W. Y.; Zhu, J.; Wen, T. B.; Yu, K. P.; Sung, H. H. Y.; Williams, I.; Lin, Z.; Jia G. *J. Am. Chem. Soc.* **2006**, *128*, 13742−13752.

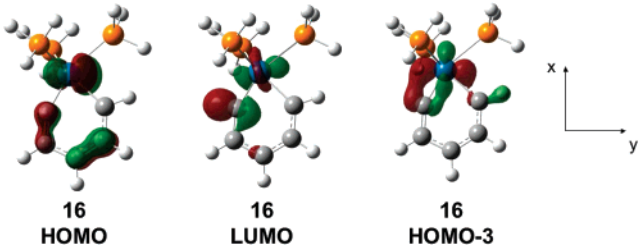

Figure 14. HOMO−3, HOMO, and LUMO of the singlet *o*-osmabenzyne **16** (isovalue for surfaces of HOMO and LUMO = 0.04; isovalue for zurfaces of HOMO−3 = 0.08). The two localized orbitals of HOMO, LUMO, and HOMO−3, occupied by α and β electrons, look the same.

of the aromaticity of this *o*-benzyne analogue, or to decide why it is so much more stable than the *para* analogue.

As Figure 14 shows, the HOMO of **16** is a π orbital of the ring (with d_π participation), whereas the LUMO has contribution from $p_{in-plane}$ of the carbon atom and $d_{x^2-y^2}$ of Os. The LUMO does look like the antibonding component of the in-plane strained third bond. Its bonding partner may be found in HOMO−3, MO49. Due to the geometry and ligands of **16**, its HOMO and LUMOs differ significantly from those of the osmabenzyne prepared by Jia.[12]

Metallabenzenes

Addition of two hydrogens to metallabenzynes **8**, **11**, and **15** generates (on paper) metallabenzenes **17**, **18**, and **19**.[51] These molecules are isolobal with benzene; thus, they are expected to exhibit aromatic properties (with all the ambiguities that surround that nicely fuzzy concept).[9,13,52] Optimized structures of **17**, **18**, and **19** are presented below.

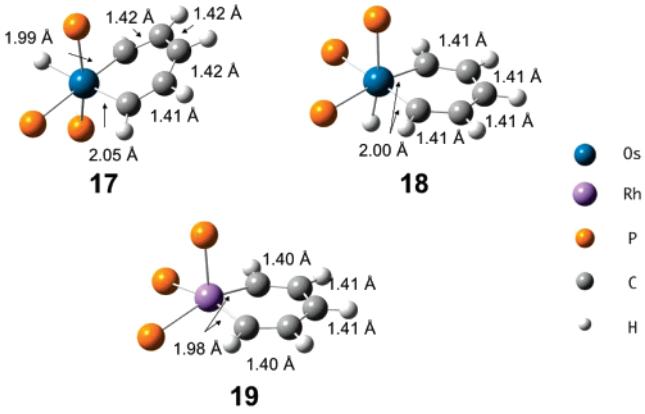

Note that osmabenzenes **17**, **18**, and **19** are slightly nonplanar, as some known metallabenzenes are.[8,13] The bond distances and bond angles computed for **17** (C_1), **18**, and **19** (both C_s) are in good agreement with experimental values from crystallographic studies of known compounds.[8,13] Note the nicely equalized CC distances. The C−Os bond distance in **17** and **18** and the C−Rh

(51) The reaction energies for the hydrogenation of metallabenzynes **8**, **11**, and **15** are given in the Supporting Information.

(52) (a) Minkin, V. I.; Glukhovtsev, M. N.; Simkin, B. Y. *Aromaticity and Antiaromaticity*; John Wiley & Sons: New York, 1994. (b) Schleyer, P. v. R.; Jiao, H. *Pure Appl. Chem.* **1996**, *68*, 209−218. (c) Lioyd, D. *J. Chem. Inf. Comput. Sci.* **1996**, *36*, 442−447. (d) Krygowski, T. M.; Cyranski, M. K.; Czarnocki, Z.; Hafelinger, G.; Katritzky, A. R. *Tetrahedron* **2000**, *56*, 1783−1796. (e) Schleyer, P. v. R., Guest Ed. *Chem. Rev.* **2001**, *101*, 1115−1566 (special issue on Aromaticity). (f) Schleyer, P. v. R., Guest Ed. *Chem. Rev.* **2005**, *105*, 3433−3947 (special issue on Delocalization−Pi and Sigma).

bond distances in **19** are 1.99 Å and 2.05 Å, 2.00 Å and 1.98 Å, respectively, not very different from each other.

Conclusions

We have studied theoretically the Bergman cyclization of three metallaenediynes, **6**, **9**, and **14**, designed by application of the isolobal analogy. We were able to decrease the computed activation energy of the Bergman cyclization to 13 kcal/mol in osmaenediyne **6**, with the corresponding end-to-end separation between acetylides *d* of 3.31 Å. In two other metallaenediynes, **9** and **14**, E_a is decreased somewhat (to 23 kcal/mol in **9**) or not at all (33 kcal/mol in **14**). Our computations indicate further that, aside from a potentially significant decrease in the energy of activation, the metalla-Bergman cyclization becomes exothermic when a 14-electron metal fragment replaces a 4-electron carbon.

The computational results suggest a new family of organometallic enediynes. One may also hope that they can be synthesized and that their biochemical properties will be of interest.

Acknowledgment. We thank Cornell University and the Ohio Supercomputer Center for providing computational resources. We are grateful to the NSF (Grant CHE 0613306) for support of this work.

Supporting Information Available: Potential energy surfaces for the rearrangement of osmaenediyne **6** computed with BLYP/SDD, B3LYP/LANL2DZ, and BLYP/LANL2DZ; optimized singlet and triplet of **8**, **8′**, **11**, **11′**, and **15** and their relative energies and $\langle S^2 \rangle$ values; HOMO and LUMO of singlet **8**, **8′**, **11**, **11′**, and **15**; energy and $\langle S^2 \rangle$ of singlet **8**, **8′**, **11**, **11′** and **15** and triplet (from singlet geometry); energy and $\langle S^2 \rangle$ of singlet (from triplet geometry) and triplet **8**, **8′**, **11**, **11′**, and **15**; computed PES for the racemization of *p*-osmabenzyne **8**; isomeric trigonal bipyramids obtained by rearranging **14** via a Berry pseudorotation; computed PES for the rearrangement of rhodaenediyne **14**; NBO charges of **3** and **8**; reaction energies for the hydrogenation of metallabenzynes **8**, **11**, and **15**; complete ref 14; and geometries, absolute energies, and number of imaginary frequencies of the stationary points presented in the paper. This material is available free of charge via the Internet at http://pubs.acs.org.

JA068884V